https://doi.org/10.1016/j.energy.2019.116213

Validations of three-dimensional wake models with the wind field measurements in complex terrain

Haiying Sun[a], Xiaoxia Gao[b], Hongxing Yang[a*]

[a]Renewable Energy Research Group, Department of Building Services Engineering, The Hong Kong Polytechnic University, Hong Kong, China
[b]Department of Power Engineering, North China Electric Power University (Baoding), China

Abstract

This paper aims to validate the analytical three-dimensional wake models by the wind data measured at a complex-terrain hilly wind farm in China. The wake models take into account the variation of wind speed in the vertical direction. The profiles of wind speeds were scanned by two moveable lidars. Two scanning modes were adopted to obtain the profiles of wind speed in vertical and horizontal directions, respectively. When validating the wake model for a single wind turbine in the vertical direction, the model can predict the wind speeds with acceptable accuracy, especially at positions beyond 10D downstream distance or above 100m height. Some large errors were found at positions less than 40m height. Wind speeds in two symmetrical side sections showed different distributions at the same downwind positions. When validating the wake model for multiple wind turbines in horizontal direction, the model also had a reliable accuracy at the far wake positions and near the inflow measuring site, but it cannot predict the wind deficits before an operating wind turbine and was not accurate in some complex-terrain situations. Suggestions and factors were given to be considered for improving the wake models in the future.

Keywords: Wake effect; Three-dimensional wake models; Wind field experiments; Validation of wake models.

1. Introduction

Energy produced from fossil fuels increases environmental damage and causes global warming [1]. Therefore, renewable energy is recently promising because of its inexhaustible and environment-friendly characteristic [2]. Wind energy is a representative renewable energy to resist the increasing global warming and pollution problems [3]. In wind farms, wake effect is a typical complex phenomenon. It affects the downstream wind turbines and the power output of the whole wind farm. Therefore, the investigation of wake effect is significant in both research and engineering areas.

Wake models have been developed and applied to handle the problems related to wind farms. In terms of optimizing the layout of a wind farm, analytical wake models were mainly adopted to estimate the wind losses caused by wake effect because of the relative simplicity and the high precision [4]. The most widely used analytical wake model is the one-dimensional (1-D) Jensen wake model, also known as the Park model [5]. It assumes that the wake expands linearly after the upstream wind turbine [6]. The calculation based on the Jensen wake model has the acceptable accuracy and the lowest computation cost among wake models [7]. However, in Jensen wake model, the inside wind velocity at any particular downstream distance is set to be constant across the wake plume, which is far from reality. Some two-dimensional (2-D)

* Corresponding author. Tel.: 2766 5863
E-mail address: hong-xing.yang@polyu.edu.hk

wake models were further developed based on the 1-D wake model. The Bastankhah wake model [8] was developed in 2014, in which the distribution of wind speed is only related to the downstream distance to the wind turbine and the distance to the hub axis. In 2015, a Cosine wake model [9] was built based on the assumption that the distribution of wind speed is cosine-shaped on the horizontal plane. On the other hand, both theoretical investigation [10] and the experiment study [11] found that the wind deficit is approximately Gaussian axisymmetric-shaped after a certain downwind distance. Therefore, in the year of 2016, Gao, et al. [12] presented a Jensen-Gaussian wake model, in which the profile of wind speed is Gaussian-shaped. The practical limitations of 2-D wake models cannot be ignored, because they do not consider the variation of wind speed in the height direction, which remains the spatial optimization problems unsolved. Authors of this paper then developed a new three-dimensional (3-D) wake model, which includes the consideration of the vertical direction [13]. The wake model has been proved to have good accuracy with some limited wind tunnel experiments. To check its applicability in real engineering, the validation with the experimental data from an operating wind farm is needed.

The early wind farm measurement can go back to the year of 1982, when a field measurement was conducted for three MOD-2 wind turbines situated at Goodnoe Hills, Washington [14]. The objective was to study the deficit of wind speed in the centerline and the development in different meteorological conditions. Later on, onshore wind farm measuring campaigns were organized with different objectives, such as experiments in Sexbierum wind farm [15], experiments in Nørrekær Enge wind farm [16], ECN Wind turbine Test station Wieringermeer [17], CWEX-10, CWEX-11 experiments [18, 19] and CWEX-13 experiments [20] in wind farm in central Iowa. Some other wake validations were focused on isolated WTs, not wind farms [21-23]. Recently, some offshore wind farm measurement campaigns were also conducted. The reason is that wind losses and enhanced loads caused by wake effect are even larger in offshore wind farms [24, 25]. Ship-mounted sodar was applied in experiments in Vindeby wind farm [26], and the results were used to evaluate several wake models [27], including Risø engineering model [28], Risø WAsP model [29], Risø analytical model [30], UO FLaP model [31], ECN Wakefarm model [32] and RGU computational fluid dynamics model [33]. Experiments were also done in Horns Rev wind farm [34] to compare various wake models. Another experiment was conducted in Middelgrunden offshore wind farm, in which two methods were described to estimate the intensity of turbulence [35]. For complex terrains, the issues of wake characterization are further enlarged [36]. On the one hand, challenge exists in describing the free stream with complex waves, turnings, and recirculation zones [37]. On the other hand, the wake behavior has a close relation to the flow as well as the terrain slope [38, 39]. Wake effect measurements have been conducted in complex-terrain Brazilian wind farms [40]. Measurements from a Norwegian wind farm have been used to validate three kinematic wake models [41]. The characteristics of wakes in complex terrains are still unveiled and not much wind field data could be used either. Advanced wind farm models based on comprehensive and accurate wake measurements are essential in the validation and development [42]. To study the 3-D wake models with the consideration of the vertical direction, the data of wind speed from full-scale complex-terrain wind farms are necessary.

In this paper, measurements of wind speed in a complex-terrain wind farm were described, and the experimental data were applied to validate the 3-D wake models. In Section 2, the 3-D wake model for a single wind turbine is introduced, and the wake model for multiple wind turbines is further developed. In Section 3, the set-up of experiments is described in details, including the information of the tested wind farm and the measuring equipment. In Section 4, two experiments of different arrangements are described. The measured wind data are applied to compare with the results from the 3-D wake models. In Section 5, the conclusions of this study are drawn. The work described herein demonstrates the effectiveness of the 3-D wake models and provides the first-hand measurements from the wind farm as well.

2. Three-dimensional wake models

A novel 3-D wake model for a single wind turbine has been presented by Sun and Yang [13]. Based on that, the 3-D wake model for multiple wind turbines has been further developed. The assumptions of the 3-D wake models are closer to reality. With the 3-D wake models, it is easy to obtain the wind velocity $U(x,y,z)$ at any position downstream of a wind turbine.

2.1 Three-dimensional wake model for a single wind turbine

The schematic diagram of the proposed 3-D wake model is shown in Figure 1. In the 3-D wake model, the wind velocity $U(x,y,z)$ is relative to the X, Y, and Z directions.

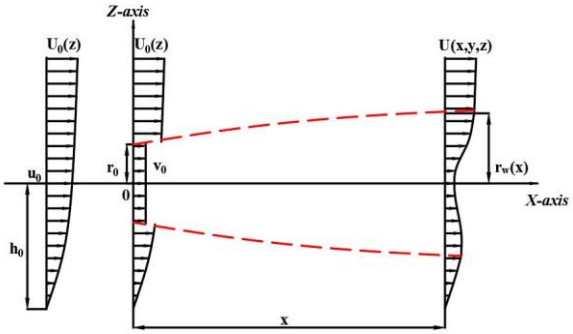

Figure 1 Schematic diagram of the 3-D wake model [13]

There are three basic assumptions about the 3-D wake model.

The first assumption is that the deficit of wind speed at the downstream distance x is Gaussian-distributed. If the incoming wind speed distribution is expressed by $U_0(z)$, the actual wind velocity $U(x,y,z)$ at the downstream position can be described by equation (1).

$$U(x,y,z)=A(x)\left(\frac{1}{2\pi\sigma(x)^2}e^{-\frac{y^2+(z-h_0)^2}{2\sigma(x)^2}}\right)+B(x)+U_0(z) \tag{1}$$

h_0 is the hub height of wind turbine. $A(x)$, $B(x)$, and $\sigma(x)$ are three important parameters that decide the Gaussian shape of the wind deficit. To simplify the calculation, $\sigma(x)$ is defined as $\sigma(x)=\frac{r_w(x)}{C}$. C is a constant and is to be determined with the real operating conditions.

The second assumption is based on the momentum conservation theory, similar to the Jensen wake model [6]. A circular area with radius $r_w(x)$ is chosen to calculate the total flow flux $Q(x)$. The expression of the second assumption is shown as equation (2).

$$\pi r_0^2 v_0+\iint_{S_{r_w(x)}-S_{r_0}}U_0(z)ds=\iint_{S_{r_w(x)}}U(x,y,z)ds \tag{2}$$

r_0 is the rotor radius of the wind turbine and v_0 is the mean wind speed just behind the wind turbine. $S_{r_x(x)}$ is the circular area with radius $r_w(x)$, and S_{r_0} is the circular area with the rotor radius r_0.

The third assumption is that the wind velocity is continuous at the wake boundary, which can be expressed by equation (3).

$$\frac{A(x)}{2\pi\sigma(x)^2}e^{-\frac{y^2+(z-h_0)^2}{2\sigma(x)^2}}+B(x)+U_0(z)=U_0(z) \quad ,where \quad y^2+(z-h_0)^2=r_w(x)^2 \tag{3}$$

Finally, $A(x)$ and $B(x)$ can be expressed by constant C as equation (4). C is an empirical parameter affected by many factors, such as the blade shape, the incoming wind speed, and the turbulence intensity. It should be set according to the real operating conditions.

$$\begin{cases} A(x)=\dfrac{Q(x)-\int_{h_0-r_w(x)}^{h_0+r_w(x)}2\sqrt{r_w(x)^2-(z-h_0)^2}\cdot U_0(z)dz}{\left(1-e^{-\frac{C^2}{2}}-\dfrac{C^2}{2}\cdot e^{-\frac{C^2}{2}}\right)} \\ B(x)=-\dfrac{A(x)\cdot C^2}{2\pi r_w(x)^2}\cdot e^{-\frac{C^2}{2}} \end{cases} \tag{4}$$

The 3-D wake model for a single wind turbine has been validated by wind tunnel experiments. Power law was adopted in the validation. The adopted horizontal wake profiles were published by reference [16]. The adopted vertical wake profile data were published by reference [43]. The log law (also known as Logarithmic Profile) [44]is adopted in this study, which is another commonly method to describe the inflow. The common expression of log law is described as equation (5).

$$U_0(z)=\frac{U^*}{k}\ln\left(\frac{z}{z_0}\right) \tag{5}$$

U^* is the friction velocity, k is the Von Kármán constant, which is recommended as 0.4 for a smooth surface, and z_0 is the surface roughness length.

2.2 Three-dimensional wake model for multiple wind turbines

The 3-D wake model then has been further developed for multiple wind turbines [45]. In this model, the first consideration is about the overlap space affected by the wake effect of more than one wind turbines. From the documentation of WindFarm software [46], the Sum of Squares method was excellent for most situations. The expression is shown as equation (6).

$$(1-\frac{u_i}{U_\infty})^2=\sum_j(1-\frac{u_{ij}}{u_j})^2 \tag{6}$$

Applying the 3-D single wake model to estimate the flow speed in the wake, the method of Sum of Squares is rewritten by equation (7).

$$[1-\frac{U_i(x,y,z)}{U_0(z)}]^2=\sum_{j=1}^{N}[1-\frac{U_{ij}(y,z)}{U_j(x,y,z)}]^2 \tag{7}$$

Next, the modification is made by applying the Sum of Squares to the equation, as shown in equation (8).

$$[U_0(z)-U_i(x,y,z)]^2=\sum_{j=1}^{N}[U_0(z)-U_{ij}(y,z)]^2 \tag{8}$$

Then, the wind distribution of the WT_i can be expressed by equation (9).

$$U_i(x,y,z)=U_0(z)-\sqrt{\sum_{j=1}^{N}[U_0(z)-U_{ij}(y,z)]^2} \tag{9}$$

If the WT_i is judged to be affected by the wake effect of other n WTs, the formula can be further specified by equation (10).

$$U_i(x,y,z) = U_0(z) - \sqrt{\sum_{j=1}^{n}[A_j(x)(\frac{1}{2\pi\sigma_j(x)^2}e^{-\frac{(y-y_j)^2+(z-h_0)^2}{2\sigma_j(x)^2}}) + B_j(x)]^2} \quad (10)$$

The 3-D wake model for multiple wind turbines has also been validated by the wind tunnel experimental data.

3. Set-up of the wind field measurements

3.1 Site and layout of Shiren wind farm

The measurements were conducted in Shiren wind farm, which is located in Shangyi Country, Zhangjiakou City, Hebei Province, China. The wind farm has a capacity of 75MW. The wind farm consists of 50 wind turbines with the rated power of 1.5MW. 33 wind turbines are the AW77-1500 type, with the rotor diameter of 77m and the hub height of 60m. Another 17 wind turbines are the UP77-1500 type, with the rotor diameter of 77m and the hub height of 65m [47]. The wind farm is built among low mountains and hilly areas. The layout of Shiren wind farm on the satellite map is shown in Figure 2.

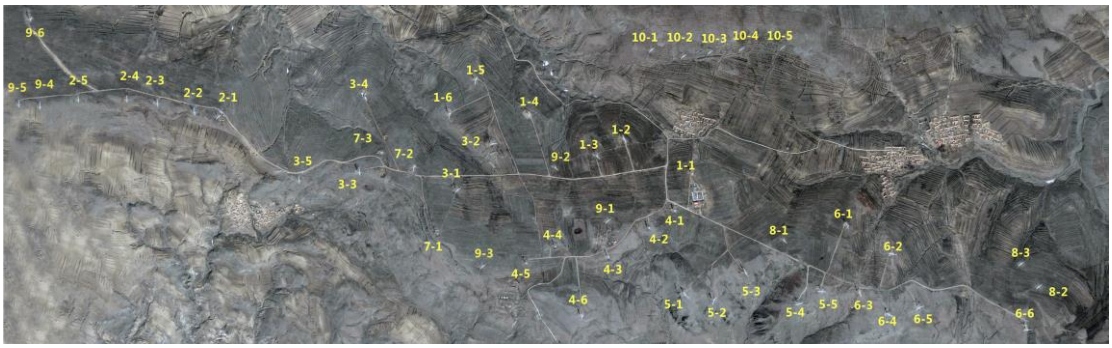

Figure 2 Layout of Shiren Wind Farm on satellite map [48]

Shiren wind farm is a good example of complex-terrain wind farms. Its largest altitude difference is 171.3 m. Among all wind turbines, the highest wind turbine is WT10-5, installed at 1894.1m high; whereas the lowest one is WT8-2, installed at 1722.8 m high. The first-hand wind speed data will contribute to both the research study and the engineering application on complex-terrain wind farms.

3.2 Measuring equipment

3.2.1 Location measuring device

To measure the locations of wind turbines and lidars accurately, a handheld was used in the experiments. Ji Si Bao G128BD is a handheld that supports Beidou, GPS and GLONASS three satellite systems perfectly. It has three power supply mode, which are dry battery, lithium battery and USB. The handheld contains electronic compass and barometer. It also supports a variety of coordinates. The handheld is shown in Figure 3.

Figure 3 Ji Si Bao G128BD Beidou handheld

3.2.2 Wind speed measuring devices

WindMast WP350 and Wind3D6000 are two lidars that were used to measure the inflow and downstream wind speeds, respectively. Both of two lidars were rented from QINGDAO Leice Transient Technology Co. LTD., and they were calibrated by the data from anemometer tower before the actual experiments. The two lidars are shown in Figure 4.

(a)

(b)

Figure 4 Measuring equipment: (a) WindMast WP350; (b) Wind3D 6000

The WindMast WP350 is a vertical-wind-mast-type lidar with a high precision. It can continuously detect wind speeds of any 30 height gates from 20 m to 350 m above it. Wind3D 6000 is 3-D scanning wind lidar. It can detect wind fields in the middle and lower troposphere. It also has the high precision, and the detection radius can be up to 6km. The technical

specifications of the two lidars are listed in Table 1.

Table 1 Technical specifications

Parameters	WindMast WP350	Wind3D6000
Wavelength	1.5μm, eye-safe	1.5μm, eye-safe
Detection height range	20m~350m	45m~6000m
Spatial resolution	30 heights in the range of 20~350m, the highest resolution is 1m	15m/30m/configurable
Data updating time / frequency	1s~10min (configurable)	1Hz~10Hz (configurable)
Wind speed range	0~75m/s	-37.5m/s~37.5m/s
Wind speed error	≤0.1m/s	≤0.1m/s
Wind direction error	<3º	±0.1º
Data product	vertical and horizontal wind speed, wind direction, mean square error of wind speed, wind shear index, SNR signal to noise ratio data, GNSS position time, radar status data, surface atmospheric temperature, humidity, pressure, etc.	DBS/VAD Wind profile, vertical flow, /RHI/PPI/CAPPI radial velocity, virtual tower stare, turbulence wake, wake vortex, wind shear, backscatter intensity, multi-lidar measurement, GNSS position, temperature humidity, pressure
Weight	<30kg	<90kg

The WindMast WP350 is suitable for wind resource exploration and assessment, wind turbine power curve test, wind power prediction, wind shear analysis, dynamics research of atmospheric boundary layer and other fields. Wind3D6000 can meet the wind measurement requirements such as complex-terrain wind field, wind turbine wake, remote virtual wind tower at sea, and stereoscopic distribution of atmospheric pollutants. Both two lidars are suitable for the experiments in this study.

4. Validations of wake models

The 3-D wake models for a single wind turbine is validated by the measurements of one wind turbine. Then the 3-D wake model for multiple wind turbines is validated by the measurements of one line of four wind turbines.

4.1 Compared with the wind speeds of a single wind turbine in vertical direction

When validating the wake model for a single wind turbine, the vertical profiles of wind speeds are representative. Therefore, Range Height Indicator (RHI) was firstly adopted in the experiments. When scanning in RHI mode, the 3D6000 holds its azimuth angle constant but varies its elevation angle. Then the returns can be mapped on a vertical plane. The elevation angle rotates in the range that covers all wake zone. In this experiment, WT10-2 was selected as the target wind turbine. The positions of wind turbines and lidars in this experiment are shown in Table 2.

Table 2 Data of wind turbines and lidars

	WT10-2	**3D6000**	**WP350**
Longitude	114.358255˚ E	114.364677˚ E	114.357298˚ E
Latitude	40.998280˚ N	40.987484˚ N	40.999399˚ N
Altitude	1884.5 m	1814.5 m	1872.3 m

The vertical profiles are from three sections, of which one is the central section and the other two are the side sections that are 39 m from the central section.

4.1.1 At the central section

A clear profile of wind speed was obtained on March 16th, 2019. The overview RHI wind speed distribution is shown in Figure 5.

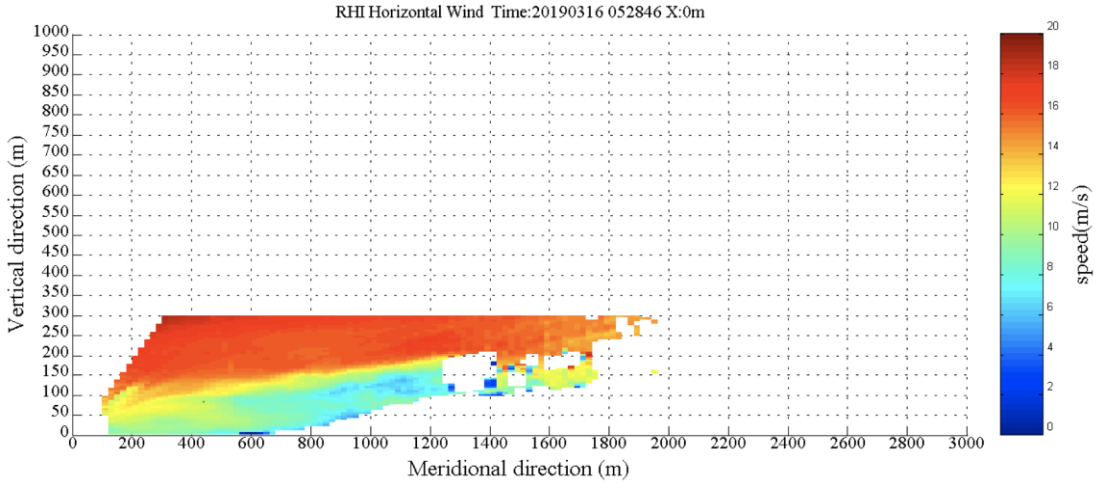

Figure 5 RHI wind speed distribution at Y=0m (time: 5:28, March 16th, 2019)

From the figure, it can be seen that WT10-2 was installed on the top of a hill. The wake developed not along the horizontal axis, but along the slope of the hill. The inflow wind speed at the measuring time is shown in Figure 6 (blue data). To calculate the wake distribution with the 3-D wake model, the incoming wind speed distribution $U_0(z)$ should be determined as accurately as possible. The simulation of inflow with the wake model is also compared in the figure.

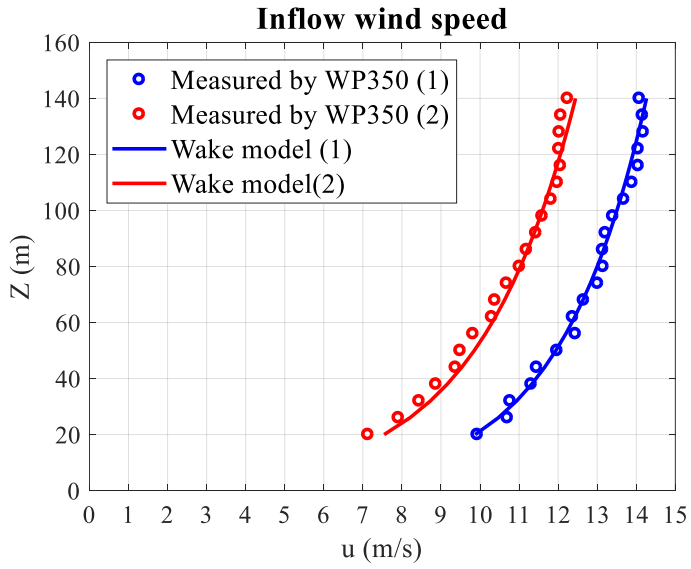

Figure 6 Inflow wind speed distribution and the simulation of 3-D wake model. (1) Time of blue data: 5:28 am to 5:29 am, March 16th, 2019. (2) Time of red data: 0:53 am to 0:54 am, March 16th, 2019

The inflow wind speed distribution simulated by the wake model fitted well with the

measured wind speed. Then comparisons of wind speeds were carried out between measurements and simulations from the 3-D wake model at a series of downstream distances. The results of the comparisons are demonstrated in Figure 7.

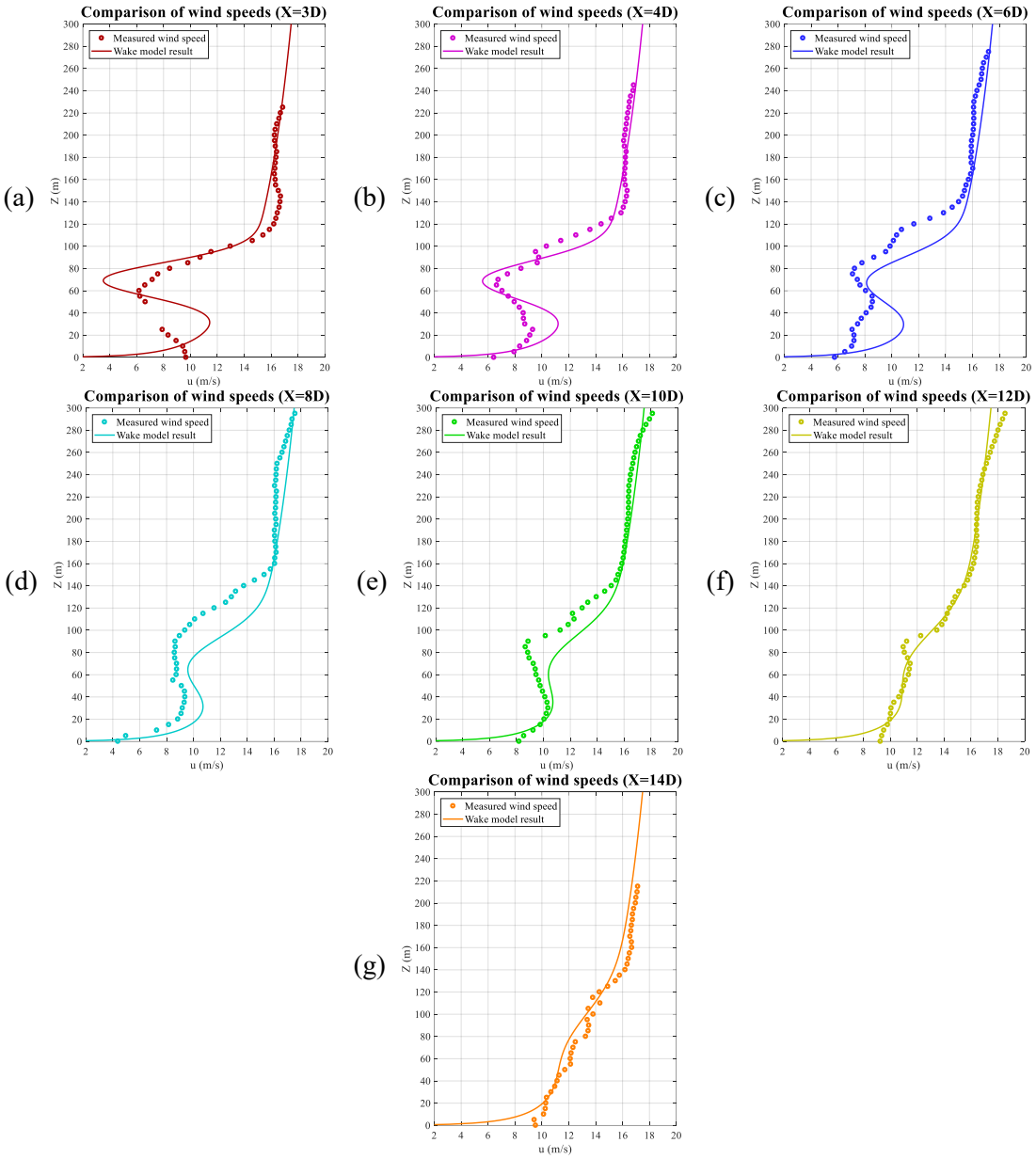

Figure 7 Comparisons of wind speeds between measurements and simulations from 3-D wake model at downstream distances of: (a) X=3D; (b) X=4D; (c) X=6D; (d) X=8D; (e) X=10D; (f) X=12D and (g) X=14D.

From comparisons, the 3-D wake model can predict the trend of wind speed in the vertical direction with the acceptable accuracy. At the positions beyond the 10D downstream distance, the 3-D wake model predicts wind speed well at all heights. Within the range from 6D to 10D, the wake model tends to overestimate wind speeds lower than the height of 140m, but predicts well above that height. In the near-wake zone, the wake model has a good accuracy where the height is over 100m. At the heights near the turbine hub, the 3-D wake model tends to underestimate wind speeds, especially right at the hub height. But it still overestimates wind speeds near the ground. The relative errors between the wake model and measurement are

shown in Figure 8.

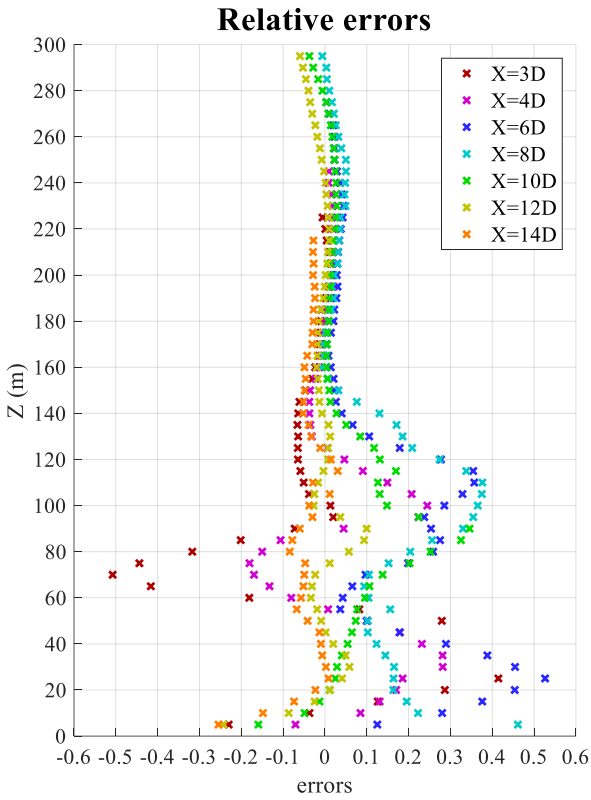

Figure 8 Relative errors between 3-D wake model and measured wind speeds at different downstream distances

As analysed before, the 3-D wake model has good accuracy in the higher positions. All relative errors are within $\pm$10% at the positions higher than 140 m. Some large errors happen at the heights smaller than 40 m, which may be because the complex turbulence effect has not been considered in the wake model. In the heights between 40 m and 100 m, the largest error is at the position of the 3D downstream distance and at the hub height, which is approximately 52%. The errors tend to be smaller with the increase of the downwind distance.

4.1.2 At the side sections

The wake model is then validated at the two side sections at the same moment of the central section comparison. The two sections are 39 m away from the central section at left and right sides, respectively. The overview RHI wind speed distributions is shown in Figure 9.

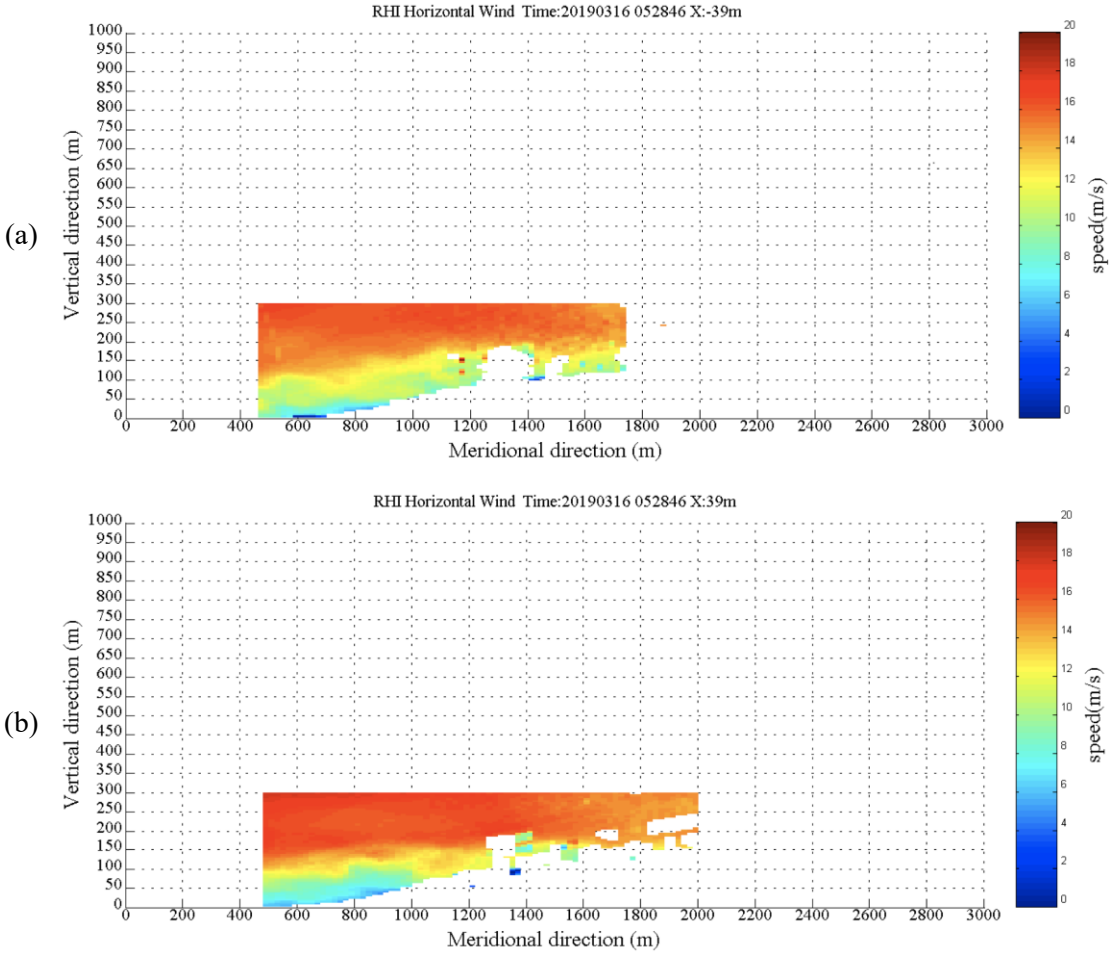

Figure 9 RHI wind speed distribution at: (a) Y=-39m, left; and (b) Y=39m, right. (time: 5:28, March 16th, 2019)

The deficits of wind speeds are not as much as those in the central section. It is worth noticing that the wind profiles at two side sections are not quite same at the moment. This is because the rotation of blades made the flow fluctuate. To study it in depth, the wind speeds at each side are compared with the wake model results. The comparisons at different downwind distances are shown in Figure 10.

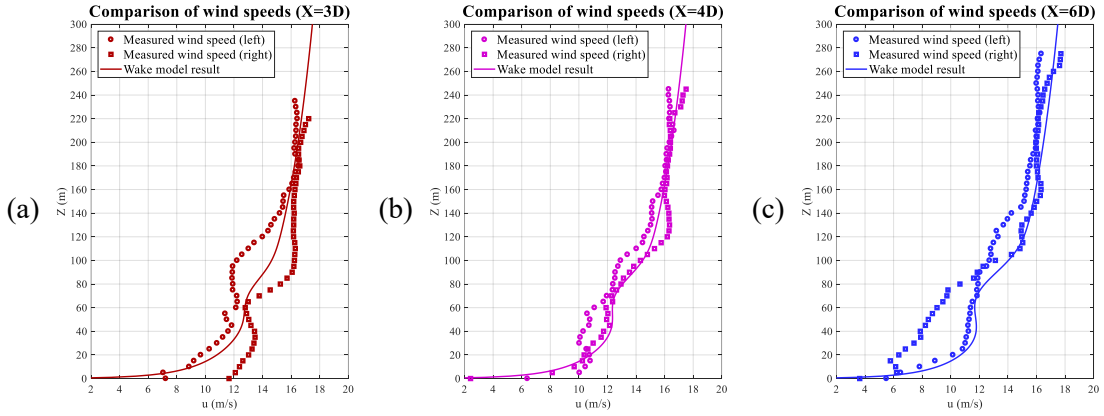

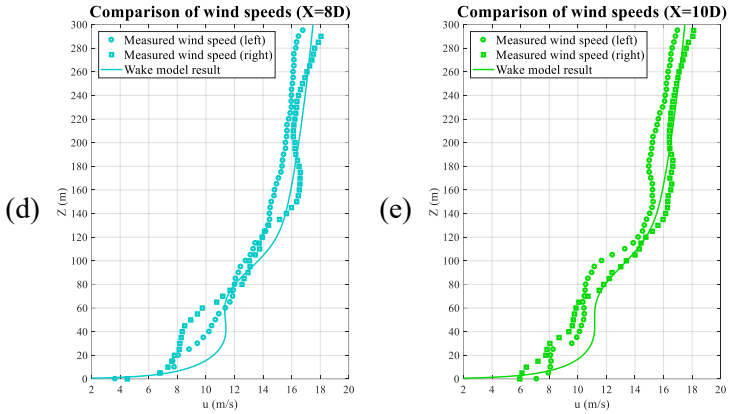

Figure 10 Comparisons of wind speeds between measurements and simulations from 3-D wake model at downstream distances of: (a) X=3D; (b) X=4D; (c) X=6D; (d) X=8D; (e) and X=10D.

From above figures, the 3-D wake model has a better agreement with the measured wind speeds at the side sections than those at the central section. Although the wind speeds at the symmetrical positions are different, the predictions from the 3-D wake model are close to the mean values of the wind speeds from two sides. The 3-D wake model still tends to overestimate wind speeds, but at a very small extent. The specific relative errors between 3-D wake model and measured wind speeds are shown in Figure 11.

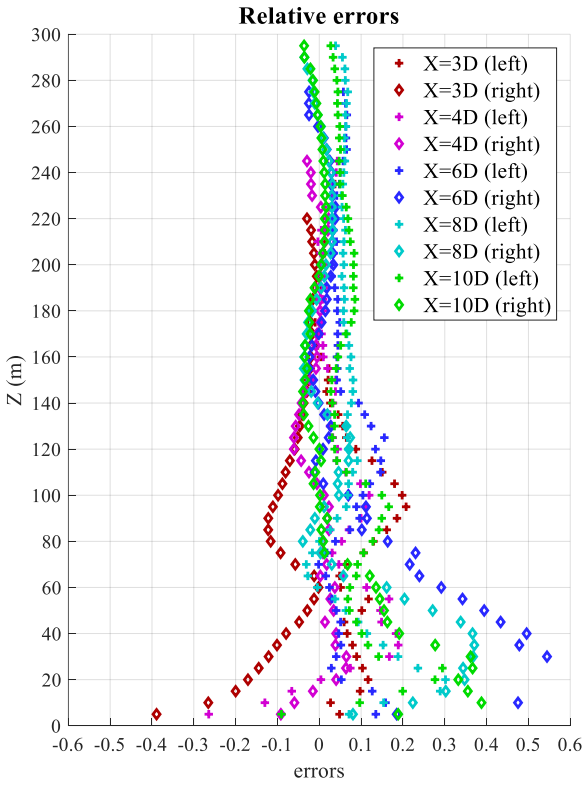

Figure 11 Relative errors between 3-D wake model and measured wind speeds at different downstream distances

Relative errors at the side sections are much smaller than those at the central section. All errors are within $\pm$30% at the positions higher than 60 m. The largest error is 54% and happens in the right section at 6D downwind distance. It is not at the hub height, but at around the 30m height, which reveals that the error is caused by the complex terrain or the turbulence near the

ground. If not consider this near-ground errors, the 3-D wake model has a good overall agreement with the measured wind speeds.

4.2 Compared with the wind speeds of multiple wind turbines in horizontal direction

The next experiment is to validate the 3-D wake model for multiple wind turbines. In this experiment, WT10-1, WT10-2, WT10-3 and WT10-4 were selected. The four wind turbines were installed almost in one line, but at various altitudes. The positions of wind turbines and lidars in this experiment are shown in Table 3.

Table 3 Data of wind turbines and lidars

	WT10-1	**WT10-2**	**WT10-3**	**WT10-4**	**3D6000**	**WP350**
Longitude	114.354838˚ E	114.358255˚ E	114.361603˚ E	114.364788˚ E	114.364677˚ E	114.357298˚ E
Latitude	40.998869˚ N	40.998280˚ N	40.998293˚ N	40.997852˚ N	40.987484˚ N	40.999399˚ N
Altitude	1857.4m	1884.5m	1880.7m	1877.3m	1814.5m	1872.3m

To investigate the interaction of wakes from multiple wind turbines at a horizontal plane, Plan Position Indicator (PPI) was applied in this plan. When scanning in PPI mode, the lidar holds its elevation angle constant, but varies its azimuth angle. The returns can then be mapped on a horizontal plane. If the lidar rotates through 360 degrees, the scan is called a *surveillance scan*. The surveillance scan is no need in this study, therefore, 3D6000 only conducted a sector scan and rotated through less than 360 degrees. The horizontal wind speed distribution at the height of 135m is shown in Figure 12.

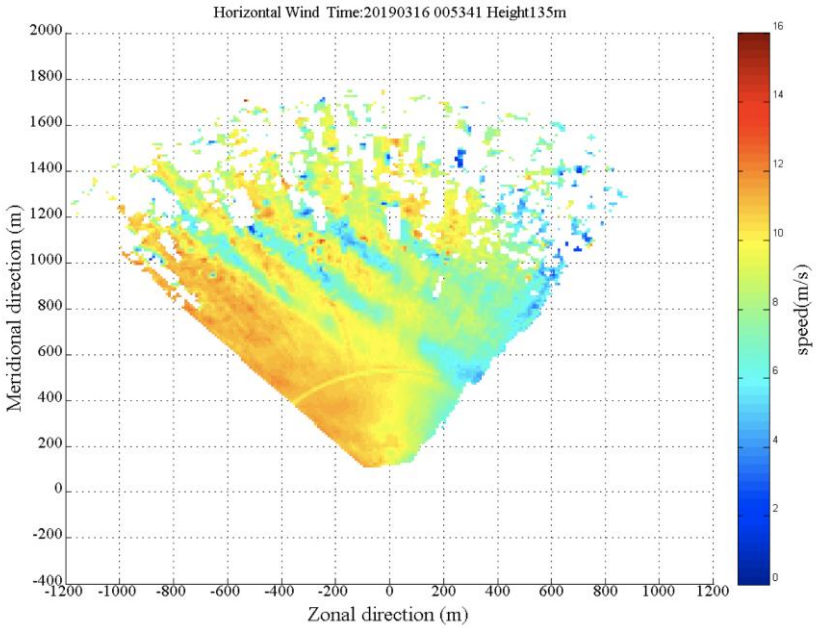

Figure 12 Horizontal wind speed distribution at the height of 135m (time: 0:53 am, March 16th, 2019)

The moment with effective results was selected when four wind turbines were operating simultaneously, and no turbine was under the wake effect of other turbines. It can be seen from the figure that wakes happen behind wind turbines and then develop along the wind direction. The wake-influenced area expands with the increase of the downstream distance. In the far-wake zone, some positions are overlapped by wakes from two upstream wind turbines simultaneously. The inflow wind speed distribution and the simulation of 3-D wake model are

shown in Figure 6 (red data).

The 3-D wake model with the log law also shows good accuracy in simulating the inflow wind speed. To quantitatively compare the results from the 3-D wake model to the measured data, some analyzing lines were set according to the wind direction. Wind speed data are filtered according to four downwind and seventeen crosswind analyzing lines, as shown in Figure 13.

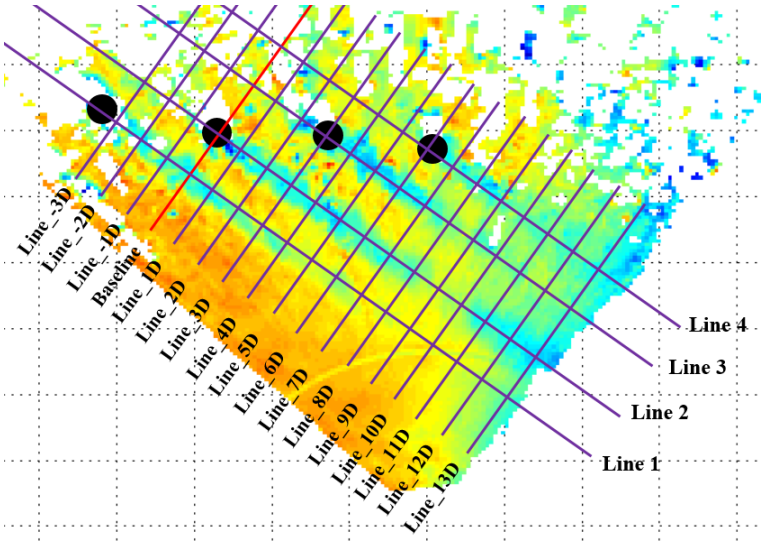

Figure 13 Diagram of analyzing lines

Line 1, Line 2, Line 3 and Line 4 are in the wind direction and go through WT10-1, WT10-2, WT10-3 and WT10-4, respectively. The Baseline goes through WT10-2 and is in the crosswind direction. Line_-3D to Line_13D are seventeen lines parallel to the Baseline and are used to analyze the wind speed in cross sections at different downstream distances of four turbines. The distance from Baseline to Line _1D is 1D. The spacing between any other two adjacent lines is 1D as well. Comparisons of wind speeds between measurements and simulations from 3-D wake model at a series of downstream distances are shown in Figure 14.

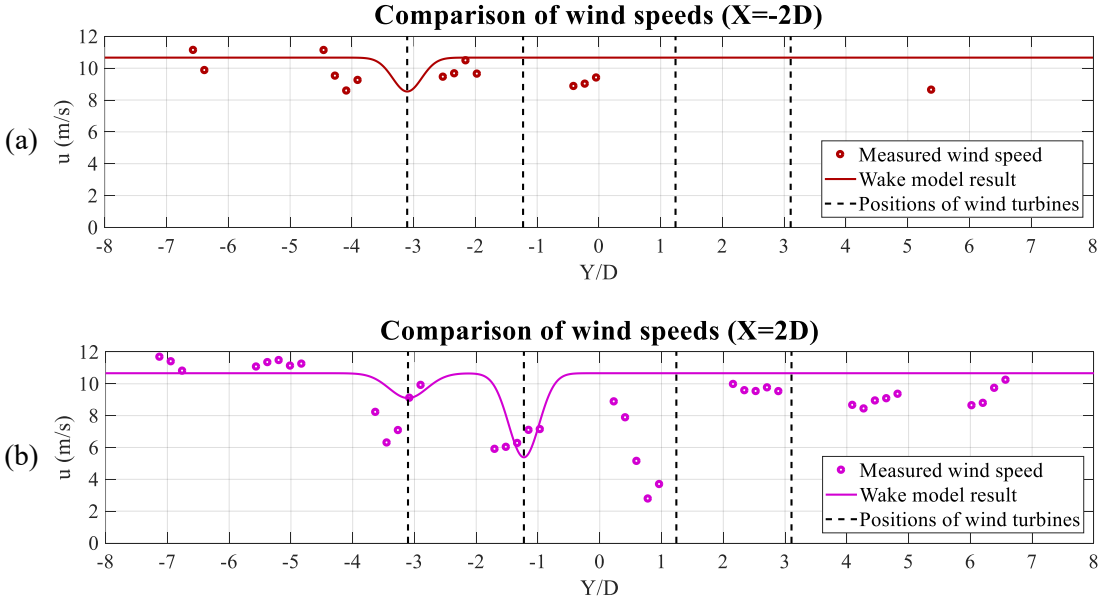

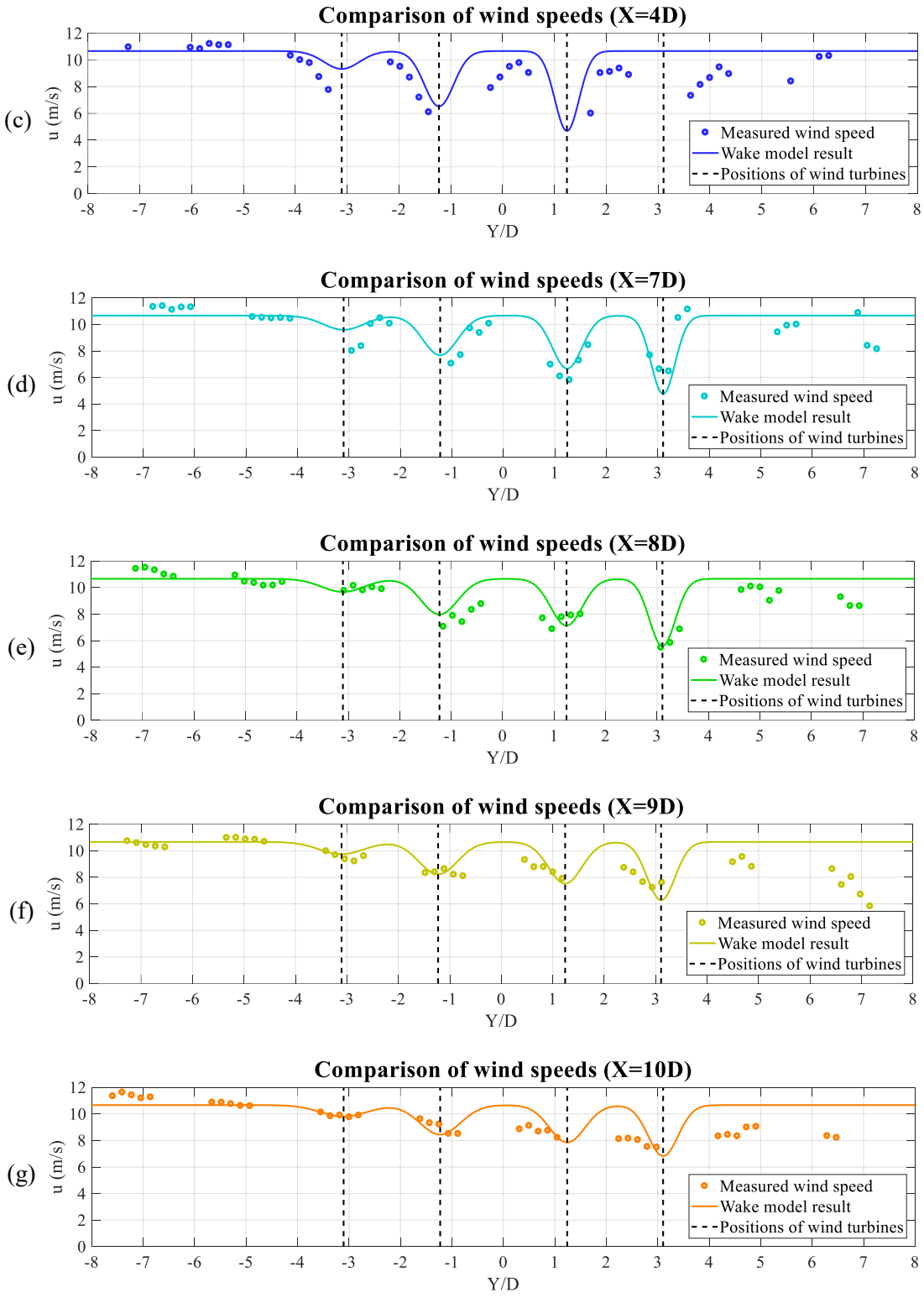

Figure 14 Comparisons of wind speeds between measurements and simulations from 3-D wake model at downstream distances of: (a) X=-2D; (b) X=2D; (c) X=4D; (d) X=7D; (e) X=8D; (f) X=9D and (g) X=10D.

With the downwind distance increasing from X=-2D to X=10D, the effect of wake interactions also becomes more obvious. The four wind turbines' wakes only affect the positions behind Line_7D. Ahead of that line, at X=-2D, X=2D and X=4D positions, wind speeds are

only influenced by wakes of one, two and three wind turbines, respectively. For Line_-2D, it is supposed to be only under the wake effect of WT10-1, however, the wind speed deficit is also observed at the positions near WT10-2. Several measured data have been obtained, but no data were on the centerline of wakes. The measurements may be not stable at that position. For Line_2D, the 3-D wake model predicts the deficit of wind speed at the positions right downwind WT10-1 and WT10-2, but could not predict the deficit before WT10-3. The similar situation also happens to Line_4D, where the 3-D wake model estimates the wind speed downwind the three left wind turbines with pretty good accuracy, but cannot predict the wind deficit before WT10-4. According to the measurements data from the first three lines, the deficit of wind speeds does not only exist behind the wind turbine, but also exists within a short distance before an operating wind turbine. This phenomenon could not be described by the 3-D wake model.

For Line_7D, Line_8D, Line_9D and Line_10D, the wakes of all four wind turbines have an influence on those positions. From the comparisons, the 3-D wake model has a reliable accuracy in predicting the wind deficits, especially in the far-wake zone. The 3-D wake model tends to estimate the wind speeds very well for positions in Line 2, which are within the wake zone of WT10-2. For Line 4, the 3-D wake model does not show relatively good estimations. The reason could be found from the environmental wind speeds. In the wake model, the inflow is determined by the measured data of WP350, which is installed near WT10-2, so the wake model shows good performance at the positions around WT10-2. For WT10-4, since it is quite far from WT10-2, the inflow may be different from that of WT10-2. This phenomenon could be seen from the environmental wind speeds on the right side of WT10-4, where the environmental wind speeds are smaller than the inflow in the wake model.

To sum up, the 3-D wake model has a good overall prediction for wind deficits influenced by multiple wind turbines. Some complicated situations exist in the complex-terrain wind farm, which makes the wake model not accurate in some positions. More factors should be considered in the wake model in the further study.

5. Conclusions

In this paper, the three-dimensional (3-D) wind turbine wake models for a single and multiple wind turbines were developed. Wind field experiments were conducted to validate the wake models and understand the wake effect in complex terrains. The main conclusions from this paper are drawn as follows:

The 3-D wake model for a single wind turbine has been further developed for multiple wind turbines, based on the Sum of Squares method. The analytical wake models could be applied to estimate the distribution of wind speeds in spatial. The inflow wind speed in the wake models could be determined with different functions to fit the distribution of the environmental wind.

Wind field measurements have been carried out in a complex-terrain wind farm in north China. Two scanning modes were adopted to validate the 3-D wake models in both vertical and horizontal planes. The experimental investigation also provided a better understanding of the wind turbine wake characteristics.

The 3-D wake models have been validated by comparing the analytical results with the measured wind speed data. From the comparisons in the vertical direction, the wake models tended to have better predictions in all high positions than those in near-ground positions. The accuracies of the models could also be improved with the increase of the downstream distance and the distance from the centerline. Comparing the wind speeds in the two symmetrical side sections, different distributions were demonstrated in the same downwind positions, which contributed to the errors of the wake models. The asymmetrical characteristics of wakes also deserve further studies.

For horizontal directions, the 3-D wake models showed good accuracies at the far wake positions and the locations near the inflow measuring site. Deficits of wind speed exist before an operating wind turbine, which could not be estimated from the wake models. In complex-terrain wind farms, the inflows of wind turbines could be different from each other. Therefore, it will cause errors of wake models if inflows of all wind turbines are assumed to be the same.

From this study, the presented 3-D wake models have a good overall agreement with the measured data from the wind farm. The complex terrain of the tested wind farm makes the inflow and the wind distribution at the near-wake zone more complicated, which may beyond the prediction of the present 3-D wake models. Therefore, involving more practical factors of complex terrain in the wake models is a very important future research field and is being investigated by the authors.

Acknowledgement

The work described in this paper was supported by the Research Institute for Sustainable Urban Development (RISUD) with account number of BBW8, the FCE Dean Research project with account number of ZVHL, The Hong Kong Polytechnic University, and National Natural Science Funds of China with grant number of 51606068.

References

[1] T. Taner, "Economic analysis of a wind power plant: A case study for the Cappadocia region," *Journal of Mechanical Science and Technology,* vol. 32, no. 3, pp. 1379-1389, 2018/03/01 2018.

[2] H. Sun, X. Gao, and H. Yang, "Investigation into offshore wind farm repowering optimization in Hong Kong," *International Journal of Low-Carbon Technologies,* vol. 14, no. 2, pp. 302-311, 2019.

[3] H. Sun, H. Yang, and X. Gao, "Investigation into spacing restriction and layout optimization of wind farm with multiple types of wind turbines," *Energy,* vol. 168, pp. 637-650, 2019/02/01/ 2019.

[4] A. Niayifar and F. Porté-Agel, "Analytical modeling of wind farms: A new approach for power prediction," *Energies,* vol. 9, no. 9, p. 741, 2016.

[5] S. F. Rodrigues, R. Teixeira Pinto, M. Soleimanzadeh, P. A. N. Bosman, and P. Bauer, "Wake losses optimization of offshore wind farms with moveable floating wind turbines," *Energy Conversion and Management,* vol. 89, pp. 933-941, 1/1/ 2015.

[6] N. O. Jensen, *A note on wind generator interaction*. 1983.

[7] R. Shakoor, M. Y. Hassan, A. Raheem, and Y.-K. Wu, "Wake effect modeling: A review of wind farm layout optimization using Jensen′s model," *Renewable and Sustainable Energy Reviews,* vol. 58, pp. 1048-1059, 5// 2016.

[8] M. Bastankhah and F. Porté-Agel, "A new analytical model for wind-turbine wakes," *Renewable Energy,* vol. 70, pp. 116-123, 10// 2014.

[9] L. L. Tian, W. J. Zhu, W. Z. Shen, N. Zhao, and Z. W. Shen, "Development and validation of a new two-dimensional wake model for wind turbine wakes," *Journal of Wind Engineering and Industrial Aerodynamics,* vol. 137, pp. 90-99, Feb 2015.

[10] N. P. Dufresne and M. Wosnik, "Velocity deficit and swirl in the turbulent wake of a wind turbine," *Marine Technology Society Journal,* vol. 47, no. 4, pp. 193-205, 2013.

[11] L. P. Chamorro and F. Porté-Agel, "A wind-tunnel investigation of wind-turbine wakes: boundary-layer turbulence effects," *Boundary-layer meteorology,* vol. 132, no. 1, pp. 129-149, 2009.

[12] X. Gao, H. Yang, and L. Lu, "Optimization of wind turbine layout position in a wind farm using a newly-developed two-dimensional wake model," *Applied Energy,* vol. 174, pp. 192-200, 2016.

[13] H. Sun and H. Yang, "Study on an innovative three-dimensional wind turbine wake model," *Applied Energy,* vol. 226, pp. 483-493, 2018/09/15/ 2018.

[14] P. B. S. Lissaman, T. G. Zambrano, and G. W. Gyatt, "Wake structure measurements at the Mod-2 cluster test facility at Goodnoe Hills," Article 1983.

[15] J. Cleijne, "Results of sexbierum wind farm: single wake measurements," 1993.

[16] W. Schlez, A. Tindal, and D. Quarton, "GH wind farmer validation report," Garrad Hassan and

Partners Ltd, Bristol,2003.
[17] L. A. H. MacHielse, P. J. Eecen, H. Korterink, S. P. Van Der Pijl, and J. G. Schepers, "ECN test farm measurements for validation of wake Models," in *European Wind Energy Conference and Exhibition 2007, EWEC 2007*, 2007, vol. 1, pp. 172-181.
[18] D. A. Rajewski *et al.*, "Crop wind energy experiment (CWEX): observations of surface-layer, boundary layer, and mesoscale interactions with a wind farm," *Bulletin of the American Meteorological Society,* vol. 94, no. 5, pp. 655-672, 2013.
[19] M. E. Rhodes and J. K. Lundquist, "The effect of wind-turbine wakes on summertime US midwest atmospheric wind profiles as observed with ground-based doppler lidar," *Boundary-Layer Meteorology,* vol. 149, no. 1, pp. 85-103, 2013.
[20] B. J. Vanderwende, J. K. Lundquist, M. E. Rhodes, E. S. Takle, and S. L. Irvin, "Observing and simulating the summertime low-level jet in central Iowa," *Monthly Weather Review,* vol. 143, no. 6, pp. 2319-2336, 2015.
[21] B. D. Hirth, J. L. Schroeder, W. S. Gunter, and J. G. Guynes, "Measuring a utility-scale turbine wake using the TTUKa mobile research radars," *Journal of Atmospheric and Oceanic Technology,* vol. 29, no. 6, pp. 765-771, 2012.
[22] M. L. Aitken, R. M. Banta, Y. L. Pichugina, and J. K. Lundquist, "Quantifying wind turbine wake characteristics from scanning remote sensor data," *Journal of Atmospheric and Oceanic Technology,* vol. 31, no. 4, pp. 765-787, 2014.
[23] Q. a. Li, T. Maeda, Y. Kamada, and N. Mori, "Investigation of wake effects on a Horizontal Axis Wind Turbine in field experiments (Part I: Horizontal axis direction)," *Energy,* vol. 134, pp. 482-492, 9/1/ 2017.
[24] R. J. Barthelmie *et al.*, "Quantifying the Impact of Wind Turbine Wakes on Power Output at Offshore Wind Farms," *Journal of Atmospheric and Oceanic Technology,* vol. 27, no. 8, pp. 1302-1317, Aug 2010.
[25] R. J. Barthelmie, K. S. Hansen, and S. C. Pryor, "Meteorological Controls on Wind Turbine Wakes," *Proceedings of the Ieee,* vol. 101, no. 4, pp. 1010-1019, Apr 2013.
[26] R. J. Barthelmie *et al.*, "Offshore wind turbine wakes measured by sodar," *Journal of Atmospheric and Oceanic Technology,* vol. 20, no. 4, pp. 466-477, Apr 2003.
[27] R. J. Barthelmie *et al.*, "Comparison of wake model simulations with offshore wind turbine wake profiles measured by sodar," *Journal of Atmospheric and Oceanic Technology,* vol. 23, no. 7, pp. 888-901, Jul 2006.
[28] G. C. Larsen, I. Carlen, and G. Schepers, "Fatigue life consumption in wake operation," in *2nd IEA Symposium on Wind Conditions for Wind Turbine Design*, 1999, pp. 77-82: Technical University of Denmark. Department of Fluid Mechanics.
[29] I. Katic, J. Højstrup, and N. O. Jensen, "A simple model for cluster efficiency," in *European wind energy association conference and exhibition*, 1986, pp. 407-410.
[30] S. Frandsen *et al.*, "Analytical modelling of wind speed deficit in large offshore wind farms," *Wind energy,* vol. 9, no. 1‐2, pp. 39-53, 2006.
[31] J. F. Ainslie, "Calculating the flowfield in the wake of wind turbines," *Journal of Wind Engineering and Industrial Aerodynamics,* vol. 27, no. 1-3, pp. 213-224, 1988.
[32] A. Crespo, J. Hernandez, E. Fraga, and C. Andreu, "Experimental validation of the UPM computer code to calculate wind turbine wakes and comparison with other models," *Journal of Wind Engineering and Industrial Aerodynamics,* vol. 27, no. 1-3, pp. 77-88, 1988.
[33] M. Magnusson, K. Rados, and S. Voutsinas, "A study of the flow downstream of a wind turbine using measurements and simulations," *Wind Engineering,* pp. 389-403, 1996.
[34] R. J. Barthelmie *et al.*, "Modelling and Measuring Flow and Wind Turbine Wakes in Large Wind Farms Offshore," *Wind Energy,* vol. 12, no. 5, pp. 431-444, Jul 2009.
[35] R. J. Barthelmie, S. T. Frandsen, M. N. Nielsen, S. C. Pryor, P. E. Rethore, and H. E. Jorgensen, "Modelling and measurements of power losses and turbulence intensity in wind turbine wakes at Middelgrunden offshore wind farm," *Wind Energy,* vol. 10, no. 6, pp. 517-528, Nov-Dec 2007.
[36] R. J. Barthelmie, S. C. Pryor, N. Wildmann, and R. Menke, "Wind turbine wake characterization in complex terrain via integrated Doppler lidar data from the Perdigao experiment," in *Journal of Physics: Conference Series*, 2018, vol. 1037.
[37] A. M. Forsting, A. Bechmann, and N. Troldborg, "A numerical study on the flow upstream of a wind turbine in complex terrain," in *Journal of Physics: Conference Series*, 2016, vol. 753, no. 3, p. 032041: IOP Publishing.
[38] E. S. Politis, J. Prospathopoulos, D. Cabezon, K. S. Hansen, P. Chaviaropoulos, and R. J. Barthelmie, "Modeling wake effects in large wind farms in complex terrain: the problem, the

methods and the issues," *Wind Energy,* vol. 15, no. 1, pp. 161-182, 2012.
[39] N. Vasiljević *et al.*, "Perdigão 2015: methodology for atmospheric multi-Doppler lidar experiments," *Atmospheric Measurement Techniques,* vol. 10, no. 9, pp. 3463-3483, 2017.
[40] G. S. Bohme, E. A. Fadigas, A. L. V. Gimenes, and C. E. M. Tassinari, "Wake effect measurement in complex terrain - A case study in Brazilian wind farms," *Energy,* vol. 161, pp. 277-283, Oct 2018.
[41] F. Seim, A. R. Gravdahl, and M. S. Adaramola, "Validation of kinematic wind turbine wake models in complex terrain using actual windfarm production data," *Energy,* vol. 123, pp. 742-753, Mar 2017.
[42] J. J. Trujillo, F. Bingöl, G. C. Larsen, J. Mann, and M. Kühn, "Light detection and ranging measurements of wake dynamics. Part II: two‐dimensional scanning," *Wind Energy,* vol. 14, no. 1, pp. 61-75, 2011.
[43] Y.-T. Wu and F. Porté-Agel, "Large-eddy simulation of wind-turbine wakes: evaluation of turbine parametrisations," *Boundary-layer meteorology,* vol. 138, no. 3, pp. 345-366, 2011.
[44] J. F. Manwell, J. G. McGowan, and A. L. Rogers, *Wind energy explained: theory, design and application*. John Wiley & Sons, 2010.
[45] H. Sun and H. Yang, "Numerical investigation of the average wind speed of a single wind turbine and development of a novel three-dimensional multiple wind turbine wake model," *Renewable Energy,* vol. 147, pp. 192-203, 2020/03/01/ 2020.
[46] E. Djerf and H. Mattsson, "Evaluation of the software program windfarm and comparisons with measured data from alsvik," *The aeronautical research institute of Sweden,* 2000.
[47] X. Gao *et al.*, "Investigation of wind turbine performance coupling wake and topography effects based on LiDAR measurements and SCADA data," *Applied Energy,* vol. 255, p. 113816, 2019/12/01/ 2019.
[48] Google Map, "Shiren Wind Farm," ed, 2018.